

# Electronic Impurity Doping in CdSe Nanocrystals

*Ayaskanta Sahu,<sup>†,‡</sup> Moon Sung Kang,<sup>‡,§,¶</sup> Alexander Kompch,<sup>§</sup> Christian Notthoff,<sup>§</sup> Andrew W. Wills,<sup>#</sup> Donna Deng,<sup>‡</sup> Markus Winterer,<sup>§</sup> C. Daniel Frisbie,<sup>†</sup> and David J. Norris<sup>\*,†</sup>*

<sup>†</sup>Optical Materials Engineering Laboratory, ETH Zurich, 8092 Zurich, Switzerland

<sup>‡</sup>Department of Chemical Engineering and Materials Science, University of Minnesota, Minneapolis, MN 55455, United States

<sup>§</sup>Department of Chemical Engineering, Soongsil University, Seoul 156-743, Korea

<sup>¶</sup>Nanoparticle Process Technology and Center for NanoIntegration Duisburg-Essen (CeNIDE), University Duisburg-Essen, D-47057 Duisburg, Germany

<sup>#</sup>Department of Chemistry, University of Minnesota, Minneapolis, MN 55455, United States

<sup>\*</sup>Corresponding author. E-mail: dnorris@ethz.ch

## Supporting Information

### 1. Materials and Methods

#### A. Chemicals and Substrates

Carbon tetrachloride (reagent grade, 99.9%), chloroform (HPLC grade,  $\geq$ 99.8%), hexadecylamine (HDA, technical grade, 90%), methanol (HPLC grade,  $\geq$ 99.9%), anhydrous methanol (99.8%), anhydrous ethanol ( $\geq$ 99.5%), octane (reagent grade, 98%), anhydrous octane ( $\geq$ 99%), selenium pellets (Se, 99.999%), tetrachloroethylene (TCE, spectrophotometric grade,  $\geq$ 99.9%), toluene (HPLC grade, 99.9%), sodium hydroxide pellets, platinum wire (99.9%), diphenylphosphine (DPP, 98%), tri-*n*-octylphosphine (TOP, technical grade, 90%), tri-*n*-octylphosphine oxide (TOPO, technical grade, 90%), hydrochloric acid (TraceSELECT®, for trace analysis, fuming,  $\geq$ 37%), and nitric acid [TraceSELECT®, for trace analysis,  $\geq$ 69.0% (T)] were purchased from Sigma Aldrich. Hexanes (ACS grade) was purchased from VWR International. Reagent alcohol (histological grade, 90% ethanol, 5% methanol, and 5% butanol) and butanol were obtained from Fisher Scientific. *n*-dodecylphosphonic acid (DDPA) was purchased from PCI Synthesis. Cadmium (II) oxide (CdO, 99.999%) and silver nitrate (AgNO<sub>3</sub>, 99.9995%) were purchased from Strem Chemicals. 1-ethyl-3-methylimidazolium bis(trifluoromethylsulfonyl)imide ([EMIM][TFSI]) was purchased from Solvent Innovation GmbH (Germany). All chemicals were used as delivered without further purification.

Circular sapphire windows, 12.7 mm (0.5") in diameter and 1.0 mm (0.040") thick, were purchased from Esco Products Inc. <100>-oriented, boron-doped silicon (Si) wafers (resistivity=0.005–0.01 Ωcm, thickness=525±25 μm) coated with 300 nm of thermal oxide (SiO<sub>2</sub>) were purchased from Silicon Valley Microelectronics.

## B. Synthesis of CdSe Nanocrystals

CdSe nanocrystals were prepared by modifying a known procedure.<sup>S1</sup> For 3-nm-diameter CdSe nanocrystals, CdO (410.0 mg, 3.2 mmol), hexadecylamine (HDA, 18.54 g, 76.8 mmol), *n*-dodecylphosphonic acid (DDPA, 1.608 g, 6.4 mmol), and tri-*n*-octylphosphine oxide (TOPO, 8.096 g, 20.9 mmol) were heated to 90 °C in a 100-ml four-neck round-bottom flask with continuous stirring. The flask was degassed under vacuum (<20 millitorr) and purged with dry N<sub>2</sub>. The degassing process was repeated at least three times to remove water and O<sub>2</sub>. The mixture was then heated to 315 °C under N<sub>2</sub>, and held at that temperature for nearly 30 minutes until the precursor solution turned clear. After stabilizing the colorless mixture at 280 °C, a mixture of 20 ml of a 0.2 M solution of Se in tri-*n*-octylphosphine (TOP, 4 mmol) and 0.3 ml of diphenylphosphine (DPP) prepared in a N<sub>2</sub>-filled glove box was rapidly injected into the reaction vessel with continuous stirring, resulting in a temperature drop to ~225 °C. The temperature was then quickly elevated to ~270 °C using a heat gun, and kept at that temperature for ~10 minutes to facilitate nanocrystal growth. The reaction vessel was cooled to ~90 °C and 40 ml of 1-butanol was added to prevent solidification of the reaction mixture. The nanocrystals were isolated by addition of methanol to induce flocculation, followed by centrifugation. The resulting precipitate yielded nanocrystals with surfaces coated by a mixture of HDA, DDPA, and TOP/TOPO.

To remove excess ligands, several additional purification steps were performed. Namely, the precipitate was redispersed in hexanes and centrifuged. The supernatant, which contained the nanocrystals was saved, and the precipitate [mostly unreacted hexadecylamine (HDA)] was redispersed in hexanes and centrifuged again to extract more nanocrystals. This process was repeated multiple times (typically 3) until all the possible nanocrystals were extracted from the precipitate into the supernatant. The dispersion was then stored overnight in a freezer (~20 °C). During this time, excess surfactant precipitated out of the dispersion and was removed by centrifugation. The supernatant was then filtered through a 0.2 μm polytetrafluoroethylene (PTFE) syringe filter, reagent alcohol was added, and the solution was centrifuged. Multiple iterations (in general two more cycles) of redispersion and precipitation using hexanes and reagent alcohol were done to obtain pure CdSe nanocrystals. Finally the nanocrystals, isolated as solid centrifuge pellets, were dried under vacuum, dispersed in toluene, filtered through a 0.2 μm PTFE syringe filter to obtain a stable colloidal dispersion and stored under ambient conditions until needed.

## C. Doping of CdSe Nanocrystals with Ag

To incorporate Ag, a typical exchange reaction heated 6 ml of a 5 mg/ml dispersion of CdSe nanocrystals in toluene to ~60 °C in a glass vial with continuous stirring. 1 ml of 0.1 M ethanolic AgNO<sub>3</sub> was combined with 1.5 ml of TOP and then added to the rapidly stirring dispersion. After ~2 minutes the reaction was quenched with ~10 ml of ethanol. The precipitated nanocrystals were isolated by centrifugation and then dispersed and isolated several times with hexanes and ethanol, respectively, to obtain a clean product. This process generates nanocrystals with ~1 Ag per particle on average.

## D. Sample Characterization

X-ray diffraction (XRD), transmission electron microscopy (TEM), inductively coupled plasma optical emission spectroscopy (ICP-OES), inductively coupled plasma mass spectroscopy (ICP-MS), ultraviolet-visible (UV-Vis) absorption spectroscopy, and fluorescence spectroscopy were used to characterize the size, shape, structure, composition, and optical properties of the doped nanocrystals.

For XRD, a Bruker-AXS microdiffractometer was utilized to collect wide-angle powder patterns (Cu-K $\alpha$ ). Samples were prepared from concentrated dispersions of CdSe nanocrystals in hexane. Films of these nanocrystals were deposited onto heavily doped Si wafers covered with a thermally grown 300-nm-thick SiO<sub>2</sub> layer.

For TEM, an FEI Tecnai G2 F30 microscope was used to image the nanocrystals with an acceleration voltage of 300 kV. Each sample was prepared by depositing a drop of a dilute dispersion of nanocrystals in hexanes onto a 400-mesh carbon-coated copper grid and allowing the solvent to evaporate at room temperature.

For optical characterization, nanocrystals were dispersed in hexanes and placed in a 1-cm-path-length quartz cuvette. Absorption spectra were obtained using a Cary 5E UV-Vis-near-infrared spectrophotometer. Photoluminescence spectra were collected with a Spex Fluorolog-2 spectrofluorometer equipped with two double monochromators (0.22 m, SPEX 1680) and a 450 W xenon lamp as the excitation source. For measurements at 10 K, the nanocrystals were deposited on sapphire flats that were mounted in a Janis continuous flow cryostat that was positioned in the sample compartment of the fluorometer.

For ICP-MS, we used a Thermo Scientific XSeries2 instrument with a hexapole collision/reaction cell. For calibration, we compared the intensities of the unknown to data from 4 multi-element standards purchased from SPEX Industries. Elements were analyzed at standard mass resolution using the helium/hydrogen collision reaction mode with kinetic energy discrimination. The mean and standard deviation were calculated from five measurements on each sample. The unknowns were introduced with an ESI PC3 (Peltier cooler) FAST system with sample loops to reduce oxide formation and carryover between samples. <sup>89</sup>Y was used as an internal standard.

For ICP-OES, we used a Thermo Scientific iCAP 6500 duo optical emission spectrometer with a simultaneous charge-induction detector. We measured each sample five times to determine the mean and standard deviation for each elemental wavelength. For calibration, we utilized NIST-traceable single or multi-element standards. To lessen matrix effects, we matched the matrix acid for all blanks, standards, and samples. We diluted each sample such that the elemental concentrations were in the linear range of the standard and detector combination. The probe and all tubing for introduction of the samples were made from Teflon and flushed for at least 45 seconds with clean matrix acid.

For both ICP-MS and ICP-OES, samples were prepared by dissolving ~1-2 mg of vacuum-dried nanocrystals in 5 ml of aqua regia (3:1 HCl:HNO<sub>3</sub>). The resulting ions were then diluted to ~100 ppm with 18 MΩ deionized water. To avoid contamination, trace-grade acids (HCl and HNO<sub>3</sub>) and HCl-leached plasticware and glassware were used.

## E. Transistor Measurements

For the thin-film transistors (TFTs), source and drain contacts (5 nm Cr / 35 nm Au) were patterned on Si/SiO<sub>2</sub> wafers using standard lift-off techniques. These wafers were then sonicated in acetone, isopropanol, and methanol (10 minutes in each), rinsed with methanol, and then transferred into a N<sub>2</sub> glove box. Films of nanocrystals were spin-coated (10 seconds at 900 rpm followed by 15 seconds at 1200 rpm) from a 20 mg/ml dispersion in anhydrous octane passed through a 0.2 μm PTFE filter, and were dried at room temperature for more than 1 hour. The films were then dipped into a 0.08 M solution of NaOH in anhydrous methanol for 10 minutes, rinsed with fresh anhydrous methanol, and finally annealed at 100 °C for 1 hour. To fill cracks formed during the chemical treatment, a second layer of nanocrystals was spin-coated and treated with NaOH, following the same procedure used for the first layer.

To ensure that the NaOH ligand exchange did not remove any dopants from the nanocrystal films,

we performed electron-probe micro analysis (EPMA) to determine the amount of Ag in the films before and after treatment with NaOH. For these EPMA measurements, we utilized a JEOL 8900R electron-probe micro analyzer with an acceleration voltage of 10 kV and a beam current of 50 nA with a 75  $\mu$ m beam diameter. Each element was analyzed in its own wavelength-dispersive spectrometer and pure metals or binary compounds were used as standards. A JEOL thin-film correction algorithm was used for the quantitative elemental analyses. Films of Ag-doped CdSe nanocrystals were spin-coated from dispersions in anhydrous octane on heavily doped Si wafers covered with a thermally grown 300-nm-thick SiO<sub>2</sub> layer. Data for EPMA was collected from 10 different points on each sample and analyzed. The results are summarized in Figure S10.

For the TFT measurements, the ion gel and Pt gate were applied on the top of the NaOH-treated nanocrystal film. The entire device fabrication was carried out in a N<sub>2</sub> glove box. Current–voltage (*I*-*V*) characteristics were measured in a Desert Cryogenics (Lakeshore) probe station with Keithley 237 and 6517A electrometers. Prior to electrical characterization, one of the probes was attached with a silver wire (25  $\mu$ m diameter) that was then treated with piranha solution to form an oxidized quasi-reference electrode (Ag/Ag<sub>2</sub>O). For capacitance–voltage (C–V) measurements on the working device, the probe station was connected to an HP 4192A LF impedance analyzer, and the voltage sweep was applied to the gate electrode while the source and drain electrodes were grounded. All the measurements were carried out under vacuum ( $\sim$ 10<sup>-6</sup> Torr).

#### F. Ion Gels

A symmetric poly(styrene-*block*-(methyl methacrylate)-*block*-styrene) (PS-PMMA-PS) triblock copolymer was synthesized, as previously described,<sup>S2</sup> with block molecular weights of M<sub>n</sub>(PS)=8.9 kg/mol and M<sub>n</sub>(PMMA)=67 kg/mol (overall polydispersity M<sub>w</sub>/M<sub>n</sub>=1.15). To prepare the ion gels, PS-PMMA-PS and 1-ethyl-3-methylimidazolium bis(trifluoromethylsulfonyl)imide [EMIM][TFSI] (1:9 by weight) were dissolved in dichloromethane (CH<sub>2</sub>Cl<sub>2</sub>). The solution was stirred overnight, and then poured into a Petri dish. Dichloromethane was slowly evaporated at room temperature for 24 hours, and the ion-gel solution was further dried under vacuum for an additional 24 hours. After complete evaporation of the solvent, transparent ion gels were formed. They were stored in a nitrogen glove box until needed.

#### G. Conductivity Measurements

Films of nanocrystals (~50 nm thick) were spin-coated onto a Si/SiO<sub>2</sub> substrate that was pre-patterned with source and drain electrodes (Cr/Au). The films were not treated with NaOH. The *I*<sub>D</sub> - *V*<sub>D</sub> (current – voltage) characteristics for the 10- $\mu$ m channel were measured under vacuum, and are shown in Figure S11. The scan rate was 750 mV/s. The conductivity was determined from the linear *I*-*V* relationship in the bias voltage range of -1.0 V to 1.0 V. As expected, the films were mostly insulating due to bulky ligands on the nanocrystal surface. The hysteresis observed between the forward and reverse scans can be explained by charge traps at the surface of the nanocrystals or in the surrounding medium.

## 2. References

- S1. Reiss, P.; Bleuse, J.; Pron, A. *Nano Lett.* **2002**, *2*, 781.
- S2. Hadjichristidis, N.; Pispas, S.; Floudas, G., *Block Copolymers*. John Wiley & Sons: Hoboken, 2003.

### 3. Figures

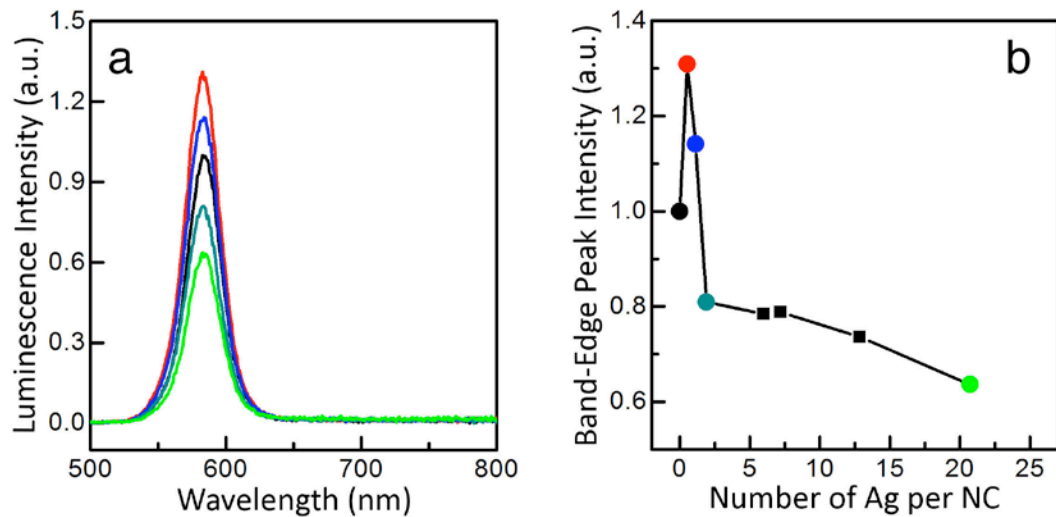


**Figure S1.** Optical characterization of 3.6-nm-diameter Ag-doped CdSe nanocrystals (NCs) dispersed in hexanes. (a) Room-temperature photoluminescence spectra of an undoped sample (black) and a series of doped samples with 0.6 Ag/NC (red), 1.1 Ag/NC (blue), 1.9 Ag/NC (dark cyan), and 20.7 Ag/NC (green). (b) Variation in the band-edge peak intensity with Ag doping. The black, red, blue, dark cyan, and green circles show the maximum fluorescence intensity for the spectra in (a). The addition of a few Ag atoms enhances the fluorescence by a factor of 1.3 and then the fluorescence slowly drops down with further doping.

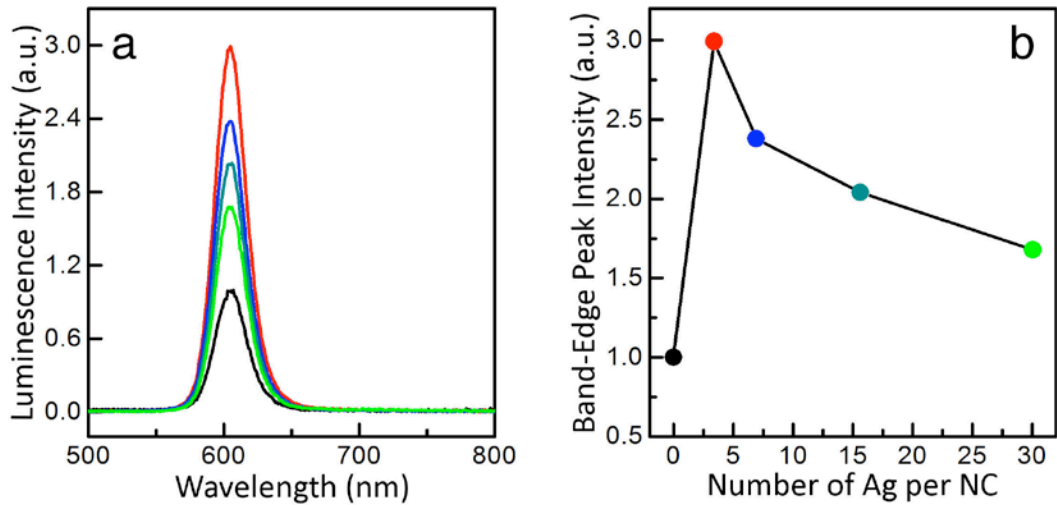


**Figure S2.** Optical characterization of 4.3-nm-diameter Ag-doped CdSe nanocrystals (NCs) dispersed in hexanes. (a) Room-temperature photoluminescence spectra of an undoped sample (black) and a series of doped samples with 3.4 Ag/NC (red), 6.9 Ag/NC (blue), 15.6 Ag/NC (dark cyan), and 30.1 Ag/NC (green). (b) Variation in the band-edge peak intensity with Ag doping for the samples in (a). The black, red, blue, dark cyan, and green circles show the maximum fluorescence intensity for the spectra in (a). The addition of a few Ag atoms enhances the fluorescence by a factor of 3 and then the fluorescence slowly drops down with further doping.

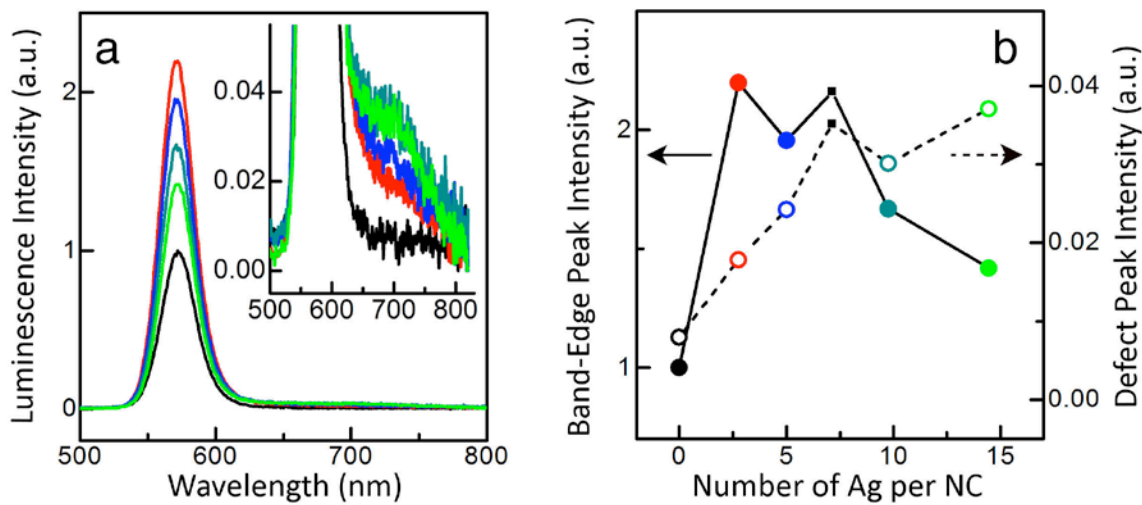


**Figure S3.** Optical characterization of 3.27-nm-diameter Ag-doped CdSe nanocrystals (NCs) dispersed in hexanes. (a) Room-temperature photoluminescence spectra of an undoped sample (black) and a series of doped samples with 2.8 Ag/NC (red), 5.0 Ag/NC (blue), 9.8 Ag/NC (dark cyan), and 14.5 Ag/NC (green). The inset shows the magnified image of a weak defect-state peak on the long-wavelength side of the band-edge peak present only in the doped samples. (b) Variation in the band-edge (solid lines and filled circles) and defect-state (dashed lines and open circles) peak intensity with Ag doping. The black, red, blue, dark cyan, and green circles show the maximum fluorescence intensity and defect-state peak intensity for the spectra in (a). The addition of a few Ag atoms enhances the band-edge fluorescence and then the fluorescence slowly drops down with further doping while the defect peak grows uniformly with doping.

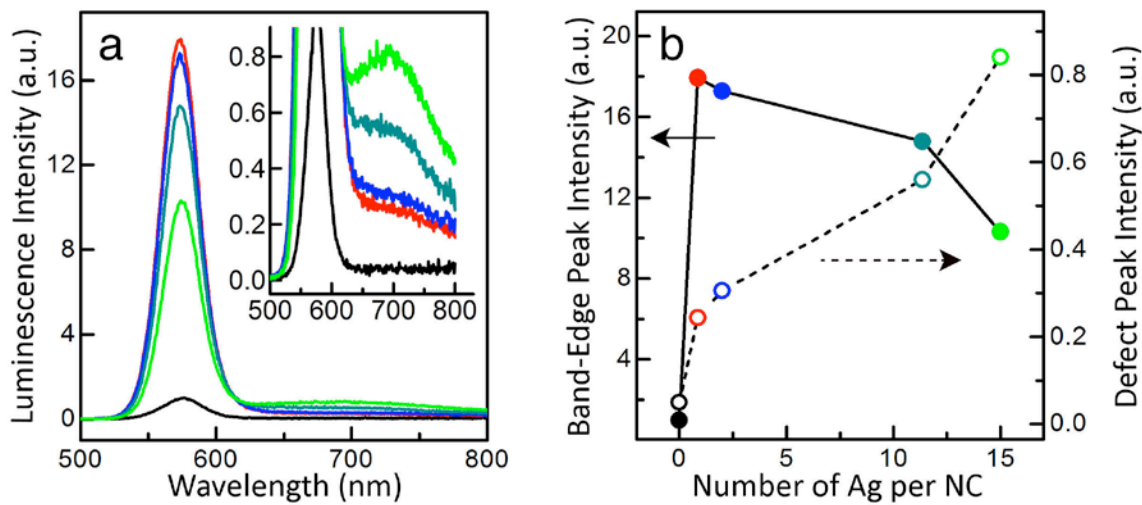


**Figure S4.** Optical characterization of 3.33-nm-diameter Ag-doped CdSe nanocrystals (NCs) dispersed in hexanes. (a) Room-temperature photoluminescence spectra of an undoped sample (black) and a series of doped samples with 0.9 Ag/NC (red), 2.0 Ag/NC (blue), 11.4 Ag/NC (dark cyan), and 15.0 Ag/NC (green). The inset shows the magnified image of a weak defect-state peak on the long-wavelength side of the band-edge peak present only in the doped samples. (b) Variation in the band-edge (solid lines and filled circles) and defect-state (dashed lines and open circles) peak intensity with Ag doping for the samples in (a). The black, red, blue, dark cyan, and green circles show the maximum fluorescence intensity and defect-state peak intensity for the spectra in (a). The addition of a few Ag atoms enhances the band-edge fluorescence and then the fluorescence slowly drops down with further doping while the defect peak grows uniformly with doping.

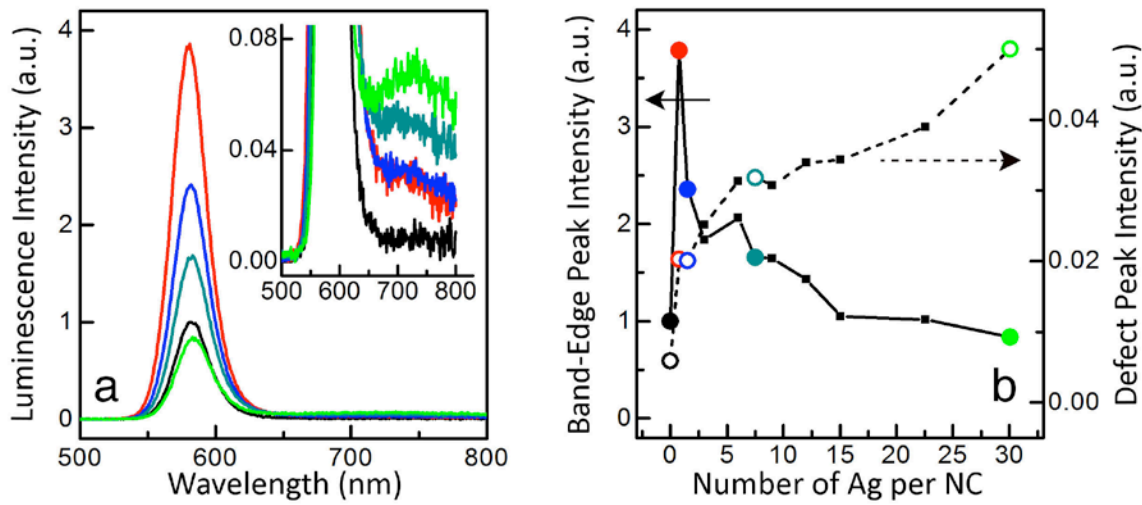


**Figure S5.** Optical characterization of 3.4-nm-diameter Ag-doped CdSe nanocrystals (NCs) dispersed in hexanes. (a) Room-temperature photoluminescence spectra of an undoped sample (black) and a series of doped samples with 0.8 Ag/NC (red), 1.5 Ag/NC (blue), 7.5 Ag/NC (dark cyan), and 30.1 Ag/NC (green). The inset shows the magnified image of a weak defect-state peak on the long-wavelength side of the band-edge peak present only in the doped samples. (b) Variation in the band-edge (solid lines and filled circles) and defect-state (dashed lines and open circles) peak intensity with Ag doping. The black, red, blue, dark cyan, and green circles show the maximum fluorescence intensity and defect-state peak intensity for the spectra in (a.) The addition of a few Ag atoms enhances the band-edge fluorescence and then the fluorescence slowly drops down with further doping while the defect peak grows uniformly with doping.

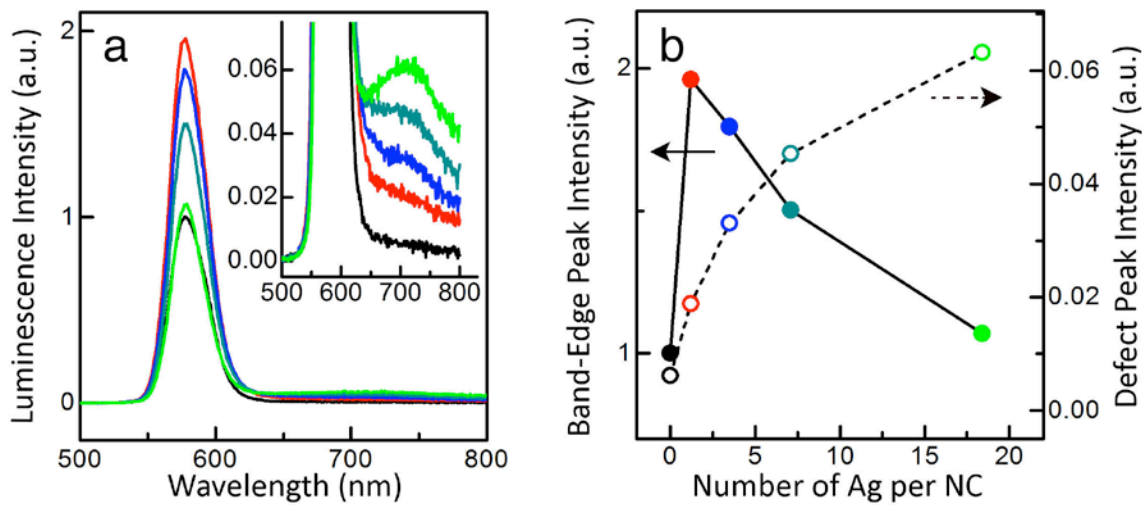


**Figure S6.** Optical characterization of 3.5-nm-diameter Ag-doped CdSe nanocrystals (NCs) dispersed in hexanes. (a) Room-temperature photoluminescence spectra of an undoped sample (black) and a series of doped samples with 1.2 Ag/NC (red), 3.5 Ag/NC (blue), 7.1 Ag/NC (dark cyan), and 18.4 Ag/NC (green). The inset shows the magnified image of a weak defect-state peak on the long-wavelength side of the band-edge peak present only in the doped samples. (b) Variation in the band-edge (solid lines and filled circles) and defect-state (dashed lines and open circles) peak intensity with Ag doping for the samples in (a). The black, red, blue, dark cyan, and green circles show the maximum fluorescence intensity and defect-state peak intensity for the spectra in (a). The addition of a few Ag atoms enhances the band-edge fluorescence and then the fluorescence slowly drops down with further doping while the defect peak grows uniformly with doping. The fluorescence quantum yield was estimated for the undoped and 1.2 Ag/NC samples. An increase from 14 to 27% was measured.

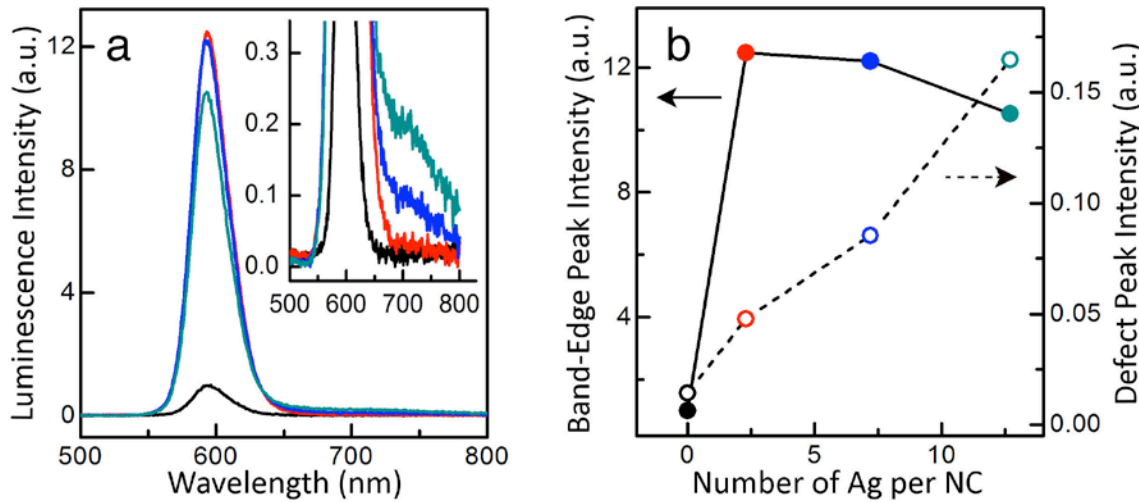


**Figure S7.** Optical characterization of 3.9-nm-diameter Ag-doped CdSe nanocrystals (NCs) dispersed in hexanes. (a) Room-temperature photoluminescence spectra of an undoped sample (black) and a series of doped samples with 2.3 Ag/NC (red), 7.2 Ag/NC (blue), and 12.7 Ag/NC (dark cyan). The inset shows the magnified image of a weak defect-state peak on the long-wavelength side of the band-edge peak present only in the doped samples. (b) Variation in the band-edge (solid lines and filled circles) and defect-state (dashed lines and open circles) peak intensity with Ag doping for the samples in (a). The black, red, blue, and dark cyan circles show the maximum fluorescence intensity and defect-state peak intensity for the spectra in (a). The addition of a few Ag atoms enhances the band-edge fluorescence and then the fluorescence slowly drops down with further doping while the defect peak grows uniformly with doping.

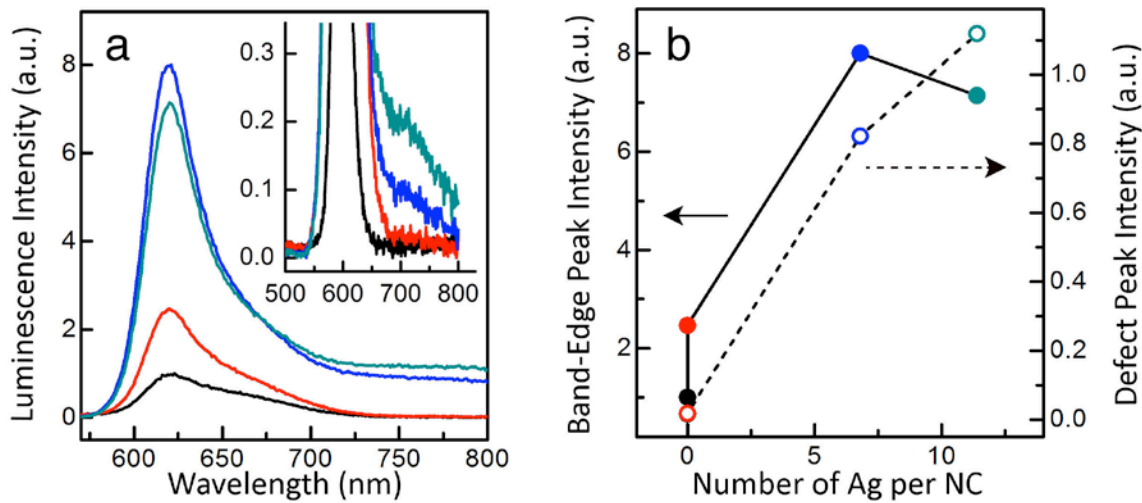


**Figure S8.** Optical characterization of 4.8-nm-diameter Ag-doped CdSe nanocrystals dispersed in hexanes with a tri-*n*-octylphosphine control experiment. (a) Room-temperature photoluminescence spectra of an undoped oleic-acid-capped CdSe nanocrystal (NC) sample (black), an undoped CdSe sample mixed with tri-*n*-octylphosphine to replicate the doping conditions (red), and two doped samples with 6.8 Ag/NC (blue) and 11.4 Ag/NC (dark cyan). The inset shows the magnified image of a weak defect-state peak on the long-wavelength side of the band-edge peak present only in the doped samples. (b) Variation in the band-edge (solid lines and filled circles) and defect-state (dashed lines and open circles) peak intensity for the samples in (a). The black, red, blue, and dark cyan circles show the maximum fluorescence intensity and defect-state peak intensity for the spectra in (a). While the addition of tri-*n*-octylphosphine enhances the band-edge fluorescence of the undoped sample, the addition of a few Ag atoms has a much greater impact on the band-edge fluorescence. Addition of tri-*n*-octylphosphine has no effect on the defect peak intensity in the undoped sample, which supports the conclusion that this feature is due to the presence of the dopants.

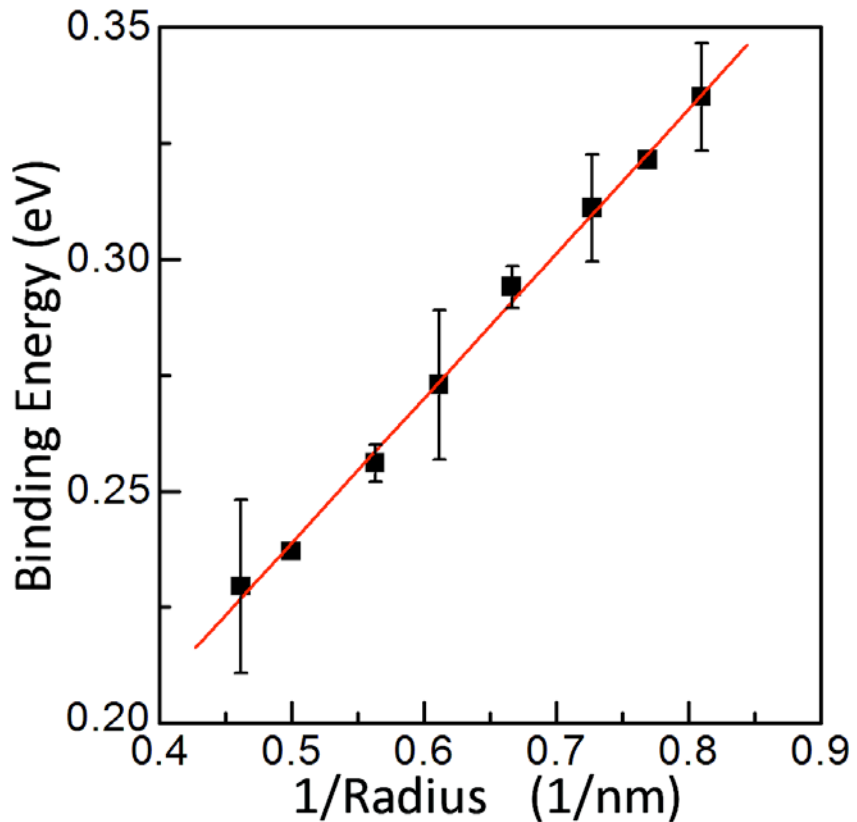


**Figure S9.** The energy separation between the band-edge emission feature and the dopant-related peak, assigned to the defect binding energy, plotted versus the inverse nanocrystal radius. The values were extracted from data as in Figure 3b from the main text for a range of nanocrystal sizes. A linear regression fit (red line) yields a coefficient of determination of 0.997. The error bars represent the standard deviation from averaging 2 to 5 samples for each size. Data points without error bars are for one sample.

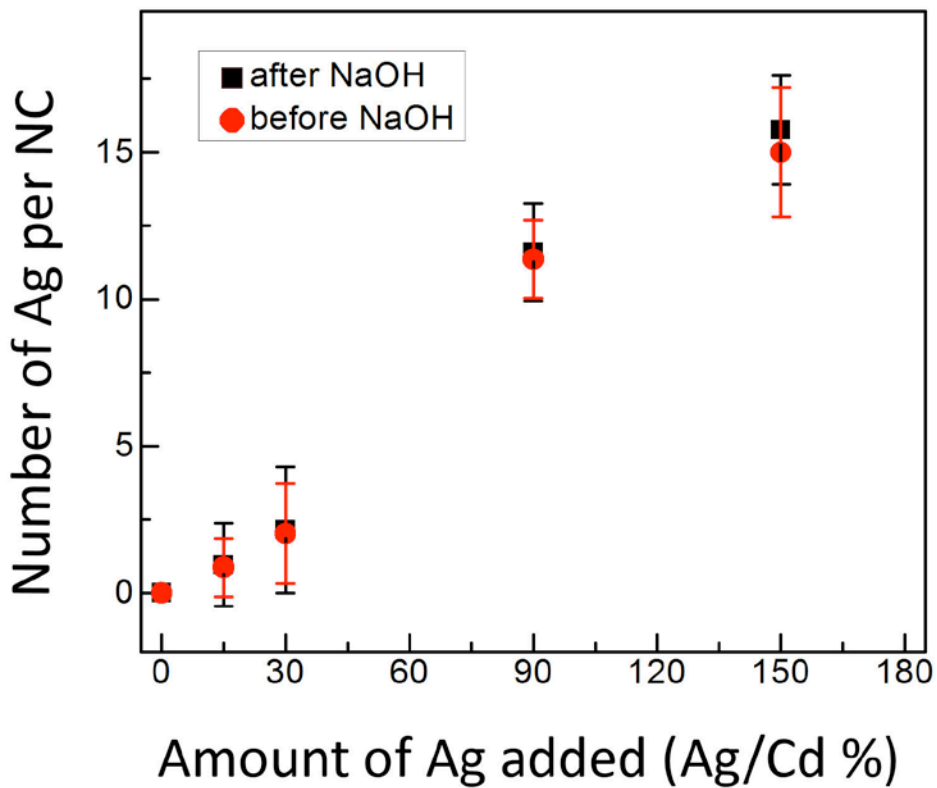


**Figure S10.** Elemental analyses of films of 3.3-nm-diameter CdSe nanocrystals. The average number of Ag atoms in the nanocrystals is plotted versus the amount of  $\text{AgNO}_3$  added to the exchange solution (as a percentage of the Cd present). Electron-probe micro analysis (EPMA) was used. The analyses were performed on devices used for electrical-transport measurements before (red circles) and after (black circles) treatment with methanolic sodium hydroxide (NaOH). The values plotted were averaged from ten measurements on different points of each sample and the error bar represents one standard deviation. The data shows no significant change in the Ag concentration in the films after the NaOH treatment.

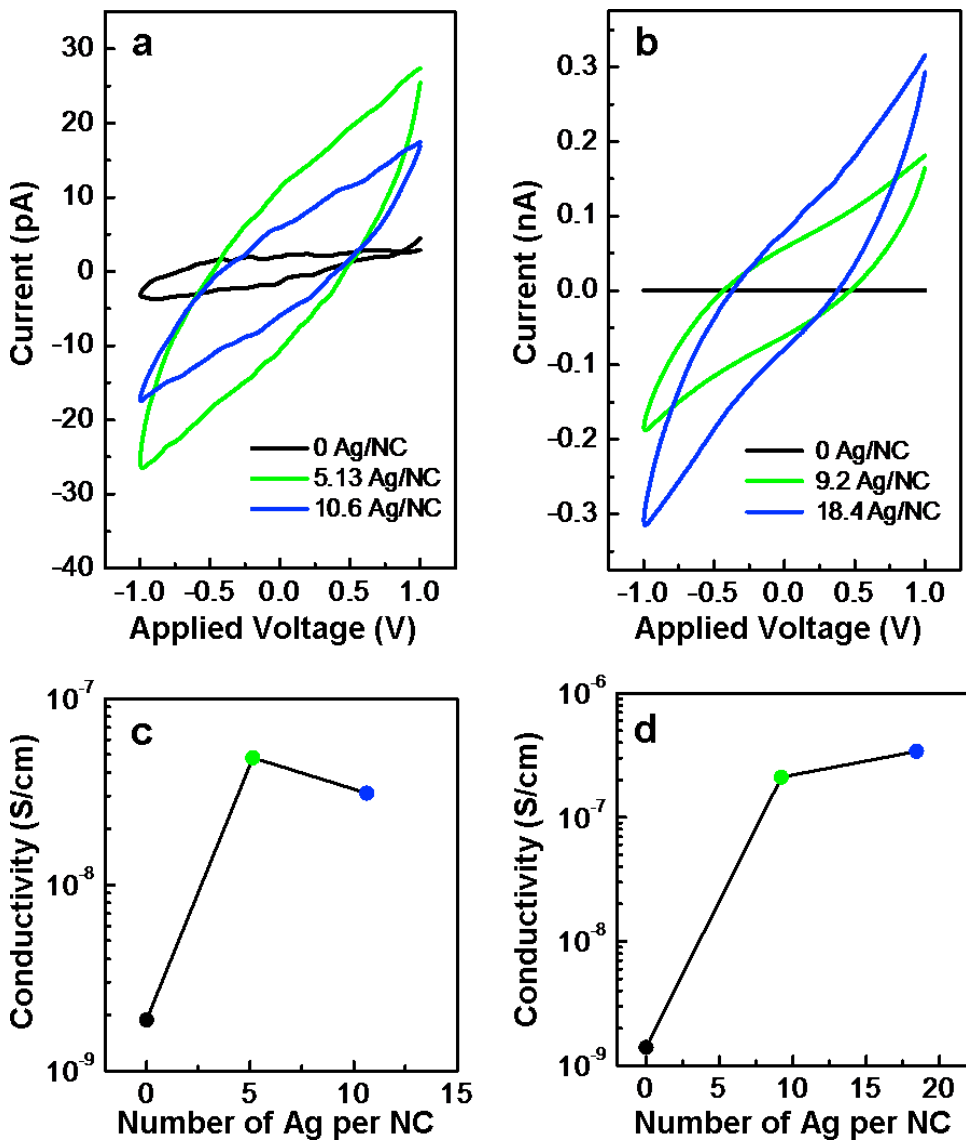


**Figure S11.** Electrical characterization of Ag-doped CdSe nanocrystals (NCs). (a) Drain current,  $I_D$ , versus the drain voltage,  $V_D$ , for 3.7-nm-diameter CdSe nanocrystals that are undoped (black) and doped with 5.13 Ag/NC (green) and 12.7 Ag/NC (blue). (b)  $I_D$  versus  $V_D$  for 4.8-nm-diameter CdSe nanocrystals that are undoped (black) and doped with 9.2 Ag/NC (green) and 18.4 Ag/NC (blue). (c) Variation in conductivity of the 3.7-nm-diameter sample in (a) with Ag doping. The black, green, and blue circles correspond to the traces in (a). (d) Variation in conductivity of the 4.8-nm-diameter sample in (b) with Ag doping. The black, green, and blue circles correspond to the traces in (b). The addition of a few Ag atoms enhances the conductivity of the NC film by  $\sim 2$  orders of magnitude.